Commun Nonlinear Sci Numer Simulat 16 (2011) 2853–2868

Contents lists available at ScienceDirect

Commun Nonlinear Sci Numer Simulat

journal homepage: www.elsevier.com/locate/cnsns

Synchronization of two different uncertain chaotic systems with unknown parameters using a robust adaptive sliding mode controller

Mohammad Pourmahmood *, Sohrab Khanmohammadi, Ghassem Alizadeh

Control Engineering Department, Faculty of Electrical and Computer Engineering, University of Tabriz, Tabriz, Iran

ARTICLE INFO

Article history:
Received 11 May 2010
Received in revised form 12 August 2010
Accepted 30 September 2010
Available online 7 October 2010

Keywords:
Sliding mode controller
Model uncertainty
External disturbance
Unknown parameter
Adaptive control

In this paper, a robust adaptive sliding mode controller (RASMC) is proposed to realize chaos synchronization between two different chaotic systems with uncertainties, external disturbances and fully unknown parameters. It is assumed that both master and slave chaotic systems are perturbed by uncertainties, external disturbances and unknown parameters. The bounds of the uncertainties and external disturbances are assumed to be unknown in advance. Suitable update laws are designed to tackle the uncertainties, external disturbances and unknown parameters. For constructing the RASMC a simple sliding surface is first designed. Then, the RASMC is derived to guarantee the occurrence of the sliding motion. The robustness and stability of the proposed RASMC is proved using Lyapunov stability theory. Finally, the introduced RASMC is applied to achieve chaos synchronization between three different pairs of the chaotic systems (Lorenz–Chen, Chen–Lorenz, and Liu–Lorenz) in the presence of the uncertainties, external disturbances and unknown parameters. Some numerical simulations are given to demonstrate the robustness and efficiency of the proposed RASMC.

1. Introduction

In the past few decades, much attention has been gained for the study of nonlinear science, especially chaos. Chaos is a particular case of nonlinear dynamics that has some specific characteristics such as extraordinary sensitivity to initial conditions and system parameter variations, broad Fourier transform spectra and fractal properties of the motion in the phase space. Due to these especial properties, chaos has been used in many practical engineering areas such as chemical reactions, power converters, secure communications, information processing, biological systems and mechanical systems [1–3] and many various control techniques have been proposed for controlling and synchronizing of chaotic systems, including sliding mode control [4–6], optimal control [7–9], adaptive control [10,11], nonlinear feedback control [12], backstepping method [13,14], passive control [15], $H\infty$ approach [16], fuzzy logic control [17], PID control [18], etc.

In addition to the control and stabilization of chaos, synchronization of chaotic systems is a fascinating concept which has been received considerable interest among nonlinear scientists in recent times. For chaos synchronization there are two chaotic systems called the master (drive) system and slave (response) system. The objective of the designed controller for synchronization is to make the output of the master system follows the output of the slave system asymptotically.

Unfortunately, most of the above mentioned works on chaos synchronization have focused on chaotic systems without model uncertainties and external disturbances in both master and slave systems. However, in practical applications, due to the modeling errors, structural variations of the systems and un-modeled dynamics uncertainties are present in the chaotic

* Corresponding author. Tel.: +98 935 8603168; fax: +98 411 3853941.
E-mail address: m.pour13@gmail.com (M. Pourmahmood).

1007-5704/$ - see front matter
doi:10.1016/j.cnsns.2010.09.038

system dynamics. Moreover, in practical situations, chaotic systems are unavoidably affected by external disturbances such as environment and measurement noises. So, synchronization of chaotic systems with uncertainties and external disturbances is effectively significant in applications. In this regard, some researchers have proposed a number of techniques for synchronization of uncertain chaotic systems that includes nonlinear feedback control [19], sliding mode control [20–24], backstepping procedure [25], linear state feedback control [26,27], active control [28] and some other methods.

However, all of the mentioned above works have a common serious drawback: they have concentrated on the synchronization of two identical chaotic systems. But, the method of the synchronization of two different chaotic systems is far from being straightforward. Also, in many real world applications, there are no exactly two identical chaotic systems. Therefore, the problem of chaos synchronization between two different uncertain chaotic systems is an important research issue. And a few researchers have developed some techniques for it that includes sliding mode control [29–31] and neural fuzzy control [32].

Nevertheless, the previous methods have studied chaotic systems with fully (or partially) known parameters. While, in practice, it is hard to exactly determine the values of the system parameters in priori. Therefore, synchronization of chaotic systems with unknown parameters is essential and useful in real-life applications. Consequently, some approaches, such as sliding mode control [33,34], finite-time based control [35], adaptive control [36–39], optimal control [40,41], fuzzy control [42–44], have been developed for synchronization of two identical chaotic systems with unknown parameters and some methods, such as adaptive control [45–49], sliding mode control [50] and backstepping method [51], have been proposed for synchronization of two different chaotic systems with unknown parameters.

In conclusion, to the best knowledge of the authors, the challenging problem of chaos synchronization between two different chaotic systems in spite of uncertainties, external disturbances and unknown parameters in both master and slave chaotic systems is not studied to this date. Therefore, the main purpose of this paper is to design a robust adaptive sliding mode controller (RASMC) to synchronize two different chaotic systems in the presence of uncertainties, external disturbances and fully unknown parameters in both master and slave chaotic systems. It is assumed that the bounds of the uncertainties and external disturbances are unknown in advance. A simple suitable sliding surface, which includes synchronization errors, is constructed. Appropriate update laws are derived to tackle the uncertainties, external disturbances and unknown parameters. Then, on the basis of the update laws, the RASMC is designed to guarantee the existence of the sliding motion. The stability and robustness of the proposed RASMC is proved using Lyapunov stability theory. Finally, three well-known chaotic systems (Lorenz, Chen, and Liu systems) are used to verify the applicability and efficiency of the introduced RASMC.

The organization of this paper is as follows. In Section 2, system description and problem formulation are presented. In Section 3, the design procedure of the proposed RASMC is given. Simulation results are included in Section 4. Finally, Section 5 ends this paper with some concluding remarks.

2. System description and problem formulation

In this paper, the n-dimensional master and slave chaotic systems with uncertainties, external disturbances and unknown parameters are given as follows:

Master system:

$$\begin{aligned}
\dot{x}_1(t) &= f_1(x_1,x_2,\ldots,x_n) + \boldsymbol{F}_1(x_1,x_2,\ldots,x_n)\boldsymbol{\theta} + \Delta f_1(x_1,x_2,\ldots,x_n,t) + d_1^m(t)\\
\dot{x}_2(t) &= f_2(x_1,x_2,\ldots,x_n) + \boldsymbol{F}_2(x_1,x_2,\ldots,x_n)\boldsymbol{\theta} + \Delta f_2(x_1,x_2,\ldots,x_n,t) + d_2^m(t)\\
&\vdots\\
\dot{x}_n(t) &= f_n(x_1,x_2,\ldots,x_n) + \boldsymbol{F}_n(x_1,x_2,\ldots,x_n)\boldsymbol{\theta} + \Delta f_n(x_1,x_2,\ldots,x_n,t) + d_n^m(t)
\end{aligned} \tag{1}$$

Slave system:

$$\begin{aligned}
\dot{y}_1(t) &= g_1(y_1,y_2,\ldots,y_n) + \boldsymbol{G}_1(y_1,y_2,\ldots,y_n)\boldsymbol{\psi} + \Delta g_1(y_1,y_2,\ldots,y_n,t) + d_1^s(t) + u_1(t)\\
\dot{y}_2(t) &= g_2(y_1,y_2,\ldots,y_n) + \boldsymbol{G}_2(y_1,y_2,\ldots,y_n)\boldsymbol{\psi} + \Delta g_2(y_1,y_2,\ldots,y_n,t) + d_2^s(t) + u_2(t)\\
&\vdots\\
\dot{y}_n(t) &= g_n(y_1,y_2,\ldots,y_n) + \boldsymbol{G}_n(y_1,y_2,\ldots,y_n)\boldsymbol{\psi} + \Delta g_n(y_1,y_2,\ldots,y_n,t) + d_n^s(t) + u_n(t)
\end{aligned} \tag{2}$$

where $\boldsymbol{x}(t) = [x_1,x_2,\ldots,x_n]^T$ is the state vector of the master system, $f_i(\boldsymbol{x})$, $i = 1,2,\ldots,n$ is a continuous nonlinear function, $\boldsymbol{F}_i(\boldsymbol{x})$, $i = 1,2,\ldots,n$ is ith row of an $n \times m$ matrix ($\boldsymbol{F}(\boldsymbol{x})$) whose elements are continuous nonlinear functions, $\boldsymbol{\theta}$ is an $m \times 1$ unknown vector parameter of the master system, $\Delta\boldsymbol{f}(\boldsymbol{x},t) = [\Delta f_1(\boldsymbol{x},t),\Delta f_2(\boldsymbol{x},t),\ldots,\Delta f_n(\boldsymbol{x},t)]^T$ and $\boldsymbol{d}^m(t) = \left[d_1^m(t),d_2^m(t),\ldots,d_n^m(t)\right]^T$ are the vectors of unknown uncertainties and external disturbances of the master system, respectively, $\boldsymbol{y}(t) = [y_1,y_2,\ldots,y_n]^T$ is the state vector of the slave system, $g_i(\boldsymbol{y})$, $i = 1,2,\ldots,n$ is a continuous nonlinear function, $\boldsymbol{G}_i(\boldsymbol{y})$, $i = 1,2,\ldots,n$ is ith row of an $n \times m$ matrix $\boldsymbol{G}(\boldsymbol{y})$ whose elements are continuous nonlinear functions, $\boldsymbol{\psi}$ is an $m \times 1$ unknown vector parameter of the slave system, $\Delta\boldsymbol{g}(\boldsymbol{y},t) = [\Delta g_1(y,t),\Delta g_2(y,t),\ldots,\Delta g_n(y,t)]^T$ and $\boldsymbol{d}^s(t) = \left[d_1^s(t),d_2^s(t),\ldots,d_n^s(t)\right]^T$ are the vectors of unknown uncertainties and external disturbances of the slave system, respectively, and $\boldsymbol{u}(t) = [u_1(t), u_2(t), \ldots, u_n(t)]^T$ is the vector of control inputs.

Assumption 1. Since the trajectories of chaotic systems are always bounded, then the unknown uncertainties $\Delta\boldsymbol{f}(\boldsymbol{x},t)$ and $\Delta\mathbf{g}(\boldsymbol{y},t)$ are assumed to be bounded. Therefore, there exist appropriate positive constants α_i^m and $\alpha_i^s,\ i = 1,2,\ldots,n$ such that

$$|\Delta f_i(\boldsymbol{x},t)| < \alpha_i^m \quad \text{and} \quad |\Delta g_i(\boldsymbol{y},t)| < \alpha_i^s, \quad i = 1,2,\ldots,n \tag{3}$$

As a result, one can conclude that

$$|\Delta f_i(\boldsymbol{x},t) - \Delta g_i(\boldsymbol{y},t)| < \alpha_i, \quad i = 1,2,\ldots,n \tag{4}$$

Assumption 2. In general, it is assumed that the external disturbances are norm-bounded in C^1, i.e.

$$\left|d_i^m(t)\right| < \beta_i^m \quad \text{and} \quad \left|d_i^s(t)\right| < \beta_i^s, \quad i = 1,2,\ldots,n. \tag{5}$$

Consequently, one can obtain that

$$\left|d_i^m(t) - d_i^s(t)\right| < \beta_i, \quad i = 1,2,\ldots,n. \tag{6}$$

Assumption 3. The constants α_i and β_i, $i = 1,2,\ldots,n$ are unknown.

To solve the synchronization problem, the error between the master system (1) and slave systems (2) can be defined as $\boldsymbol{e}(t) = \boldsymbol{x}(t) - \boldsymbol{y}(t)$. Then with subtracting Eq. (2) from Eq. (1) the error dynamics is obtained as follows:

$$\begin{aligned}
\dot{e}_1(t) &= f_1(\boldsymbol{x}) + \boldsymbol{F}_1(\boldsymbol{x})\boldsymbol{\theta} + \Delta f_1(\boldsymbol{x},t) + d_1^m(t) - g_1(\boldsymbol{y}) - \boldsymbol{G}_1(\boldsymbol{y})\boldsymbol{\psi} - \Delta g_1(\boldsymbol{y},t) - d_1^s(t) - u_1(t)\\
\dot{e}_2(t) &= f_2(\boldsymbol{x}) + \boldsymbol{F}_2(\boldsymbol{x})\boldsymbol{\theta} + \Delta f_2(\boldsymbol{x},t) + d_2^m(t) - g_2(\boldsymbol{y}) - \boldsymbol{G}_2(\boldsymbol{y})\boldsymbol{\psi} - \Delta g_2(\boldsymbol{y},t) - d_2^s(t) - u_2(t)\\
&\vdots\\
\dot{e}_n(t) &= f_n(\boldsymbol{x}) + \boldsymbol{F}_n(\boldsymbol{x})\boldsymbol{\theta} + \Delta f_n(\boldsymbol{x},t) + d_n^m(t) - g_n(\boldsymbol{y}) - \boldsymbol{G}_n(\boldsymbol{y})\boldsymbol{\psi} - \Delta g_n(\boldsymbol{y},t) - d_n^s(t) - u_n(t)
\end{aligned} \tag{7}$$

It is clear that the synchronization problem can be transformed to the equivalent problem of stabilizing the error system (7). The objective of this paper is that for any given master chaotic system (1) and slave chaotic system (2) with the uncertainties, external disturbances and unknown parameters a suitable feedback control law $\boldsymbol{u}(t)$ is designed such that the asymptotical stability of the resulting error system (7) can be achieved in the sense that $\lim_{t\to\infty}\|\boldsymbol{e}(t)\| = 0$ or equivalently $\boldsymbol{x}(t) \to \boldsymbol{y}(t)$ as $t \to \infty$.

3. Design of robust adaptive sliding mode controller

Sliding mode control [52] is a robust control method which has many interesting features such as low sensitivity to external disturbances and robustness to the plant uncertainties due to structural variations and un-modeled dynamics. The sliding mode controller is composed of an equivalent control part that describes the behavior of the system when the trajectories stay over the sliding surface and a variable structure control part that enforces the trajectories to reach the sliding surface and remain on it evermore. Adaptive control is a suitable approach to overcome system uncertainties, especially uncertainties derived from uncertain parameters. Adaptive sliding mode control has the advantages of combining the robustness of the sliding mode control with the tracking facilities of the adaptive control.

As a result, the RASMC technique includes two major steps to achieve synchronization of two different chaotic systems with uncertainties, external disturbances and unknown parameters. The first step is to select an appropriate sliding surface with the desired behavior. Therefore, the sliding surface suitable for the application can be designed as:

$$s_i(t) = \lambda_i e_i(t), \quad i = 1,2,\ldots,n \tag{8}$$

where $s_i(t) \in \boldsymbol{R}$ ($s(t) = [s_1(t), s_2(t), \ldots, s_n(t)]$) and the sliding surface parameters λ_i are positive constants.

Having established the suitable sliding surface, the next step is to determine an input signal $\boldsymbol{u}(t)$ to guarantee that the error system trajectories reach to the sliding surface $\boldsymbol{s}(t) = 0$ (i.e. to satisfy the reaching condition $\boldsymbol{s}(t)\dot{\boldsymbol{s}}(t) < 0$) and stay on it, forever. Therefore, to ensure the existence of the sliding motion a discontinuous control law is proposed as:

$$u_i(t) = f_i(\boldsymbol{x}) - g_i(\boldsymbol{y}) + \boldsymbol{F}_i(\boldsymbol{x})\hat{\boldsymbol{\theta}} - \boldsymbol{G}_i(\boldsymbol{y})\hat{\boldsymbol{\psi}} + (\hat{\alpha}_i + \hat{\beta}_i)sgn(s_i) + k_i sgn(s_i), i = 1,2,\ldots,n \tag{9}$$

where $\hat{\boldsymbol{\theta}},\ \hat{\boldsymbol{\psi}},\ \hat{\alpha}_i$ and $\hat{\beta}_i$ are estimations for $\boldsymbol{\theta}$, $\boldsymbol{\psi}$, α_i and β_i, respectively. $k_i > 0$, $i = 1,2,\ldots,n$ is the switching gain and a constant.

To tackle the uncertainties, external disturbances and unknown parameters, appropriate update laws are defined as:

$$\begin{aligned}
&\dot{\hat{\boldsymbol{\theta}}} = [\boldsymbol{F}(\boldsymbol{x})]^T\boldsymbol{\gamma}, \quad \hat{\boldsymbol{\theta}}(0) = \hat{\boldsymbol{\theta}}_0 \\
&\dot{\hat{\boldsymbol{\psi}}} = -[\boldsymbol{G}(\boldsymbol{y})]^T\boldsymbol{\gamma}, \quad \hat{\boldsymbol{\psi}}(0) = \hat{\boldsymbol{\psi}}_0 \\
&\dot{\hat{\alpha}}_i = \lambda_i|s_i|, \quad \hat{\alpha}_i(0) = \hat{\alpha}_{i0} \\
&\dot{\hat{\beta}}_i = \lambda_i|s_i|, \quad \hat{\beta}_i(0) = \hat{\beta}_{i0}
\end{aligned} \tag{10}$$

where $\boldsymbol{\gamma} = [\lambda_1 s_1, \lambda_2 s_2, \ldots, \lambda_n s_n]^T$, and $\hat{\boldsymbol{\theta}}_0$, $\hat{\boldsymbol{\psi}}_0$, $\hat{\alpha}_{i0}$ and $\hat{\beta}_{i0}$ are the initial values of the update parameters $\hat{\boldsymbol{\theta}}$, $\hat{\boldsymbol{\psi}}$, $\hat{\alpha}_i$ and $\hat{\beta}_i$, respectively.

Based on the control input in (9) and update laws in (10), to guarantee the reaching condition $\boldsymbol{s}(t)\dot{\boldsymbol{s}}(t) < 0$ and to ensure the occurrence of the sliding motion a theorem is proposed and proved. Before proceeding to the theorem, the Barbalat lemma is presented.

Lemma 1 (*Barbalat lemma [53]*). *If ω: $R \to R$ is a uniformly continuous function for $t \geqslant 0$ and if the limit of the integral*

$$\lim_{t\to\infty} \int_0^t \omega(\lambda)d\lambda \tag{11}$$

exists and is finite, then

$$\lim_{t\to\infty} \omega(t) = 0 \tag{12}$$

Theorem 1. *Consider the error dynamics (7), this system is controlled by **u**(t) in (9) with update laws in (10). Then the error system trajectories will converge to the sliding surface **s**(t) = 0.*

Proof. Selecting a positive definite function as a Lyapunov function candidate in the form of and $V(t) = \frac{1}{2}\sum_{i=1}^n \left[s_i^2 + (\hat{\alpha}_i - \alpha_i)^2 + (\hat{\beta}_i - \beta_i)^2\right] + \frac{1}{2}\|\hat{\boldsymbol{\theta}} - \boldsymbol{\theta}\|^2 + \frac{1}{2}\|\hat{\boldsymbol{\psi}} - \boldsymbol{\psi}\|^2$ taking its derivative with respect to time, one has

$$\dot{V}(t) = \sum_{i=1}^n \left[s_i\dot{s}_i + (\hat{\alpha}_i - \alpha_i)\dot{\hat{\alpha}}_i + (\hat{\beta}_i - \beta_i)\dot{\hat{\beta}}_i\right] + (\hat{\boldsymbol{\theta}} - \boldsymbol{\theta})^T\dot{\hat{\boldsymbol{\theta}}} + (\hat{\boldsymbol{\psi}} - \boldsymbol{\psi})^T\dot{\hat{\boldsymbol{\psi}}} \tag{13}$$

Since $\dot{s}_i = \lambda_i\dot{e}_i$, so replacing $\dot{e}_i$ from (7) into the above equation, we have

$$\begin{aligned}
\dot{V}(t) = &\sum_{i=1}^n \left[\lambda_i s_i(f_i(\boldsymbol{x}) + \boldsymbol{F}_i(\boldsymbol{x})\boldsymbol{\theta} + \Delta f_i(\boldsymbol{x}, t) + d_i^m(t) - g_i(\boldsymbol{y}) - \boldsymbol{G}_i(\boldsymbol{y})\boldsymbol{\psi} - \Delta g_i(\boldsymbol{y}, t) - d_i^s(t) - u_i(t)) + (\hat{\alpha}_i - \alpha_i)\dot{\hat{\alpha}} + (\hat{\beta}_i - \beta_i)\dot{\hat{\beta}}_i\right] \\
&+ (\hat{\boldsymbol{\theta}} - \boldsymbol{\theta})^T\dot{\hat{\boldsymbol{\theta}}} + (\hat{\boldsymbol{\psi}} - \boldsymbol{\psi})^T\dot{\hat{\boldsymbol{\psi}}}
\end{aligned} \tag{14}$$

Introducing update laws in (10) into the right side of Eq. (14), one obtains

$$\begin{aligned}
\dot{V}(t) = &\sum_{i=1}^n \Big[\lambda_i s_i(f_i(\boldsymbol{x}) + \boldsymbol{F}_i(\boldsymbol{x})\boldsymbol{\theta} + \Delta f_i(\boldsymbol{x}, t) + d_i^m(t) - g_i(\boldsymbol{y}) - \boldsymbol{G}_i(\boldsymbol{y})\boldsymbol{\psi} - \Delta g_i(\boldsymbol{y}, t) - d_i^s(t)) - s_i\lambda_i u_i(t) \\
&+ (\hat{\alpha}_i - \alpha_i)\lambda_i|s_i| + (\hat{\beta}_i - \beta_i)\lambda_i|s_i|\Big] + (\hat{\boldsymbol{\theta}} - \boldsymbol{\theta})^T[\boldsymbol{F}(\boldsymbol{x})]^T\boldsymbol{\gamma} - (\hat{\boldsymbol{\psi}} - \boldsymbol{\psi})^T[\boldsymbol{G}(\boldsymbol{y})]^T\boldsymbol{\gamma}
\end{aligned} \tag{15}$$

Using the facts $\sum_{i=1}^n \lambda_i s_i \boldsymbol{F}_i(\boldsymbol{x})\boldsymbol{\theta} = \boldsymbol{\theta}^T[\boldsymbol{F}(\boldsymbol{x})]^T\boldsymbol{\gamma}$ and $\sum_{i=1}^n \lambda_i s_i \boldsymbol{G}_i(\boldsymbol{y})\boldsymbol{\psi} = \boldsymbol{\psi}^T[\boldsymbol{G}(\boldsymbol{y})]^T\boldsymbol{\gamma}$, one has

$$\begin{aligned}
\dot{V}(t) = &\sum_{i=1}^n \left[\lambda_i s_i(f_i(\boldsymbol{x}) + \Delta f_i(\boldsymbol{x}, t) + d_i^m(t) - g_i(\boldsymbol{y}) - \Delta g_i(\boldsymbol{y}, t) - d_i^s(t)) - s_i\lambda_i u_i(t) + (\hat{\alpha}_i - \alpha_i)\lambda_i|s_i| + (\hat{\beta}_i - \beta_i)\lambda_i|s_i|\right] \\
&+ \hat{\boldsymbol{\theta}}^T[\boldsymbol{F}(\boldsymbol{x})]^T\boldsymbol{\gamma} - \hat{\boldsymbol{\psi}}^T[\boldsymbol{G}(\boldsymbol{y})]^T\boldsymbol{\gamma}
\end{aligned} \tag{16}$$

Substituting $u_i(t)$ from (9) into (16), this yields

$$\begin{aligned}
\dot{V}(t) = &\sum_{i=1}^n \Big[\lambda_i s_i(f_i(\boldsymbol{x}) + \Delta f_i(\boldsymbol{x}, t) + d_i^m(t) - g_i(\boldsymbol{y}) - \Delta g_i(\boldsymbol{y}, t) - d_i^s(t)) - s_i\lambda_i\Big(f_i(\boldsymbol{x}) - g_i(\boldsymbol{y}) + \boldsymbol{F}_i(\boldsymbol{x})\hat{\boldsymbol{\theta}} - \boldsymbol{G}_i(\boldsymbol{y})\hat{\boldsymbol{\psi}} \\
&+ (\hat{\alpha}_i + \hat{\beta}_i)sgn(s_i) + k_i sgn(s_i)\Big) + (\hat{\alpha}_i - \alpha_i)\lambda_i|s_i| + (\hat{\beta}_i - \beta_i)\lambda_i|s_i|\Big] + \hat{\boldsymbol{\theta}}^T[\boldsymbol{F}(\boldsymbol{x})]^T\boldsymbol{\gamma} - \hat{\boldsymbol{\psi}}^T[\boldsymbol{G}(\boldsymbol{y})]^T\boldsymbol{\gamma}
\end{aligned} \tag{17}$$

It is clear that

$$\begin{aligned}
\dot{V}(t) \leqslant &\sum_{i=1}^n \Big[\lambda_i|s_i|(|\Delta f_i(\boldsymbol{x}, t) - \Delta g_i(\boldsymbol{y}, t)| + |d_i^m(t) - d_i^s(t)|) - s_i\lambda_i\Big(\boldsymbol{F}_i(\boldsymbol{x})\hat{\boldsymbol{\theta}} - \boldsymbol{G}_i(\boldsymbol{y})\hat{\boldsymbol{\psi}} + (\hat{\alpha}_i + \hat{\beta}_i)sgn(s_i) + k_i sgn(s_i)\Big) \\
&+ (\hat{\alpha}_i - \alpha_i)\lambda_i|s_i| + (\hat{\beta}_i - \beta_i)\lambda_i|s_i|\Big] + \hat{\boldsymbol{\theta}}^T[\boldsymbol{F}(\boldsymbol{x})]^T\boldsymbol{\gamma} - \hat{\boldsymbol{\psi}}^T[\boldsymbol{G}(\boldsymbol{y})]^T\boldsymbol{\gamma}
\end{aligned} \tag{18}$$

By Assumptions 1 and 2, one can obtain

$$\dot{V}(t) \leqslant \sum_{i=1}^{n}\left[\lambda_i|s_i|(\alpha_i+\beta_i) - s_i\lambda_i\Big(\boldsymbol{F}_i(\boldsymbol{x})\hat{\boldsymbol{\theta}} - \boldsymbol{G}_i(\boldsymbol{y})\hat{\boldsymbol{\psi}} + (\hat{\alpha}_i+\hat{\beta}_i)sgn(s_i) + k_i sgn(s_i)\Big) + (\hat{\alpha}_i-\alpha_i)\lambda_i|s_i| + (\hat{\beta}_i-\beta_i)\lambda_i|s_i|\right] + \hat{\boldsymbol{\theta}}^T[\boldsymbol{F}(\boldsymbol{x})]^T\boldsymbol{\gamma} - \hat{\boldsymbol{\psi}}^T[\boldsymbol{G}(\boldsymbol{y})]^T\boldsymbol{\gamma} \tag{19}$$

It is obvious that

$$\dot{V}(t) \leqslant \sum_{i=1}^{n}\left[-s_i\lambda_i\Big(\boldsymbol{F}_i(\boldsymbol{x})\hat{\boldsymbol{\theta}} - \boldsymbol{G}_i(\boldsymbol{y})\hat{\boldsymbol{\psi}} + (\hat{\alpha}_i+\hat{\beta}_i)sgn(s_i) + k_i sgn(s_i)\Big) + \hat{\alpha}_i\lambda_i|s_i| + \hat{\beta}_i\lambda_i|s_i|\right] + \hat{\boldsymbol{\theta}}^T[\boldsymbol{F}(\boldsymbol{x})]^T\boldsymbol{\gamma} - \hat{\boldsymbol{\psi}}^T[\boldsymbol{G}(\boldsymbol{y})]^T\boldsymbol{\gamma} \tag{20}$$

By the facts $\sum_{i=1}^{n}s_i\lambda_i\boldsymbol{F}_i(\boldsymbol{x})\hat{\boldsymbol{\theta}} = \hat{\boldsymbol{\theta}}^T[\boldsymbol{F}(\boldsymbol{x})]^T\boldsymbol{\gamma}$ and $\sum_{i=1}^{n}s_i\lambda_i\boldsymbol{G}_i(\boldsymbol{y})\hat{\boldsymbol{\psi}} = \hat{\boldsymbol{\psi}}^T[\boldsymbol{G}(\boldsymbol{y})]^T\boldsymbol{\gamma}$, one has

$$\dot{V}(t) \leqslant \sum_{i=1}^{n}\left[-s_i\lambda_i\Big((\hat{\alpha}_i+\hat{\beta}_i)sgn(s_i) + k_i sgn(s_i)\Big) + \hat{\alpha}_i\lambda_i|s_i| + \hat{\beta}_i\lambda_i|s_i|\right] \tag{21}$$

Replacing $sgn(s_i)$ by $|s_i|/s_i$ into Eq. (21), this yields

$$\dot{V}(t) \leqslant \sum_{i=1}^{n} -(\hat{\alpha}_i+\hat{\beta}_i)\lambda_i|s_i| - k_i\lambda_i|s_i| + \hat{\alpha}_i\lambda_i|s_i| + \hat{\beta}_i\lambda_i|s_i| \tag{22}$$

It is apparent that

$$\dot{V}(t) \leqslant -\sum_{i=1}^{n}k_i\lambda_i|s_i| = -\sum_{i=1}^{n}\eta_i|s_i| = -\boldsymbol{\eta}|\boldsymbol{s}| \tag{23}$$

where $\eta_i = k_i\lambda_i$, $i = 1,2,\ldots,n$, $\eta = [\eta_1\eta_2,\ldots,\eta_n] > 0$ and $|\boldsymbol{s}| = [|s_1|,|s_2|,\ldots,|s_n|]^T$. Therefore $\dot{V}(t)$ becomes

$$\dot{V}(t) = -\boldsymbol{\eta}|\boldsymbol{s}| = -\omega(t) \leqslant 0 \tag{24}$$

where $\omega(t) = \boldsymbol{\eta}|\boldsymbol{s}| \geqslant 0$. Integrating Eq. (24) from zero to t yields

$$V(0) \geqslant V(t) + \int_0^t \omega(\lambda)d\lambda \tag{25}$$

Since $\dot{V}(t) \leqslant 0, V(0) - V(t) \geqslant 0$ is positive and finite and that results $\lim_{t\to\infty}\int_0^t \omega(\lambda)d\lambda$ exists and is finite (i.e. $\lim_{t\to\infty}\int_0^t \omega(\lambda)d\lambda = V(0) - V(t) \geqslant 0$). Thus, according to the Barbalat lemma, it can be obtained that

$$\lim_{t\to\infty}\omega(t) = \lim_{t\to\infty}\boldsymbol{\eta}|\boldsymbol{s}| = 0 \tag{26}$$

Since $\boldsymbol{\eta}$ is greater than zero, (26) implies $\boldsymbol{s} = 0$. Thus the proof is achieved completely. □

Remark 1. Since the control law (9) contains the *sign* function as a hard switcher, the undesirable chattering phenomenon occurs. In order to chattering reduction, the $\tanh(\varepsilon s_i)$ function, $(\varepsilon > 0)$ is replaced by the *sgn* function in (9). Therefore, the final control input becomes:

$$u_i(t) = f_i(\boldsymbol{x}) - g_i(\boldsymbol{y}) + \boldsymbol{F}_i(\boldsymbol{x})(\hat{\boldsymbol{\theta}}) - \boldsymbol{G}_i(\boldsymbol{y})\hat{\boldsymbol{\psi}} + (\hat{\alpha}_i+\hat{\beta}_i)sgn(s_i) + k_i\tanh(\varepsilon s_i), \quad i = 1,2,\ldots,n \tag{27}$$

Remark 2. Replacing the $\tanh(\varepsilon s_i)$ function by the $sign(s_i)$ function in (9) has no effect on the robustness and stability of the RASMC.

Before proving Remark 2, an auxiliary lemma is provided.

Lemma 2. *For every given scalar a and positive scalar b the following inequality holds:*

$$a\tanh(ab) = |a\tanh(ab)| = |a||\tanh(ab)| \geqslant 0 \tag{28}$$

.

Proof. From the mathematical definition of $\tanh(a)$, one has

$$a\tanh(ab) = x\frac{e^{ab} - e^{-ab}}{e^{ab} + e^{-ab}} \tag{29}$$

Multiplying above equation by $\frac{e^{ab}}{e^{ab}}$, it yields

$$a\tanh(ab) = \left(\frac{1}{e^{2ab}+1}\right)a(e^{2ab}-1) \tag{30}$$

Since $\begin{cases}(e^{2ab-1}) \geqslant 0 & \text{if } a \geqslant 0,\\ (e^{2ab-1}) < 0 & \text{if } a < 0,\end{cases}$ one can obtain

$$a(e^{2ab}-1) \geqslant 0 \tag{31}$$

Since $\left(\frac{1}{e^{2ab}+1}\right) > 0$ and from (31), one has

$$a\tanh(ab) = \left(\frac{1}{e^{2ab}+1}\right)a(e^{2ab}-1) \geqslant 0 \tag{32}$$

Therefore, from the fact that for every scalars z and v, if $zv \geqslant 0$ then $zv = |zv| = |z||v| \geqslant 0$ holds, one can conclude that

$$a\tanh(ab) = |a\tanh(ab)| = |a||\tanh(ab)| \geqslant 0 \tag{33}$$

and the proof is completed. □

Proof of Remark 2. Consider the Lyapunov function introduced in the Theorem 1. Replacing the $\tanh(\varepsilon s_i)$ function by the *sgn* function in (9) has no effect on the Eqs. (13)–(21). Therefore, from Eq. (22) one obtains

$$\dot{V}(t) \leqslant -\sum_{i=1}^{n}[-\lambda_i k_i s_i \tanh(\varepsilon s_i)] \tag{34}$$

From lemma 2 and knowing that $\lambda_i k_i > 0$, $i = 1,2,\ldots,n$, one has

$$\dot{V}(t) \leqslant -\sum_{i=1}^{n}[-\lambda_i k_i s_i \tanh(\varepsilon s_i)] = -\sum_{i=1}^{n} -\lambda_i k_i \tanh(\varepsilon s_i)||s_i| = -\sum_{i=1}^{n}\zeta_i|s_i| = -\zeta|\boldsymbol{s}| \tag{35}$$

where $\xi_i = \lambda_i k_i|\tanh(\varepsilon s_i)|$, $i = 1,2,\ldots,n$ is greater than zero and is equal to zero only when $s_i = 0$, $i = 1,2,\ldots,n$ and $\boldsymbol{\zeta} = [\zeta_1,\zeta_2,\ldots,\zeta_n]$. Therefore $\dot{V}(t)$ becomes

$$\dot{V}(t) = -\zeta|\boldsymbol{s}| = -\omega(t) \leqslant 0 \tag{36}$$

Consequently, according to the Barbalat lemma, it can be concluded that $\boldsymbol{s} = 0$. Hence the proof is completed. □

Remark 3. Theorem 1 is also valid for the chaos synchronization between two identical chaotic systems with different initial conditions, uncertainties, external disturbances and unknown parameters, if systems (1) and (2) satisfy $f_i(\boldsymbol{x}) = g_i(\boldsymbol{y})$ and $F_i(\boldsymbol{x}) = G_i(\boldsymbol{y})$, $i = 1,2,\ldots,n$.

4. Numerical simulations

In this section, some numerical simulations are presented to validate the efficiency and effectiveness of the proposed RASMC. Numerical simulations are carried out using the MATLAB software. The ode45 solver is used for solving differential equations. The Lorenz [54], Chen [55], and Liu [56] systems are three well-known chaotic systems whose nonlinear equations are given by

$$\text{Lorenz}: \begin{cases}\dot{x}_1 = 10(x_2 - x_1)\\ \dot{x}_2 = 28x_1 - x_2 - x_1x_3\\ \dot{x}_3 = x_1x_3 - 8/3x_3\end{cases} \tag{37}$$

$$\text{Chen}: \begin{cases}\dot{y}_1 = 35(y_2 - y_1)\\ \dot{y}_2 = 28y_2 - 7y_1 - y_1y_3\\ \dot{y}_3 = y_1y_3 - 3y_3\end{cases} \tag{38}$$

$$\text{Liu}: \begin{cases}\dot{z}_1 = 10(z_2 - z_1)\\ \dot{z}_2 = 40z_1 - z_1z_3\\ \dot{z}_3 = -2.5z_3 + 4z_1^2\end{cases} \tag{39}$$

In this study, three different pairs of chaotic systems (Lorenz–Chen, Chen–Lorenz, and Liu–Lorenz) are synchronized using the proposed RASMC. In all cases, $0.6\cos t$ and $-0.6\cos t$ disturbances are attached to the master and slave systems, respectively. And the following uncertainties are added to the drive and response systems, respectively.

$$\begin{cases} \Delta f_1 = 0.5\sin(\pi x_1) \\ \Delta f_2 = 0.5\sin(2\pi x_2) \\ \Delta f_3 = 0.5\sin(3\pi x_3) \end{cases} \tag{40}$$

and

$$\begin{cases} \Delta g_1 = -0.5\sin(\pi y_1) \\ \Delta g_2 = -0.5\sin(2\pi y_2) \\ \Delta g_3 = -0.5\sin(3\pi y_3) \end{cases} \tag{41}$$

In the following examples, the vectors [0.25,0.25,0.25], [0.5,0.5,0.5], [2,2,2] and [1,1,1] are selected as the initial values of the update vector parameters $\hat{\boldsymbol{\alpha}}$, $\hat{\boldsymbol{\beta}}$, $\hat{\boldsymbol{\theta}}$ and $\hat{\boldsymbol{\psi}}$, respectively. And, the coefficient ε is set to 100. Furthermore, The vector of switching gains k_1, k_2, k_3 is chosen equal to [10,10,10].

4.1. Chaos synchronization between Lorenz and Chen systems with uncertainties, external disturbances and unknown parameters

To demonstrate the efficiency of the proposed RASMC in synchronizing the Lorenz and Chen systems with uncertainties, external disturbances and unknown parameters it is assumed that the Lorenz system drives the Chen system. The master and slave systems can be rewritten in the form of Eqs. (1) and (2) as follows:

$$\dot{\boldsymbol{x}} = \underbrace{\begin{bmatrix} 0 \\ -x_1x_3 - x_2 \\ x_1x_2 \end{bmatrix}}_{\boldsymbol{f}(\boldsymbol{x})} + \underbrace{\begin{bmatrix} x_2 - x_1 & 0 & 0 \\ 0 & x_1 & 0 \\ 0 & 0 & -x_3 \end{bmatrix}}_{\boldsymbol{F}(\boldsymbol{x})} \underbrace{\begin{bmatrix} 10 \\ 28 \\ 8/3 \end{bmatrix}}_{\boldsymbol{\theta}} + \underbrace{\begin{bmatrix} 0.5\sin(\pi x_1) \\ 0.5\sin(2\pi x_2) \\ 0.5\sin(3\pi x_3) \end{bmatrix}}_{\Delta\boldsymbol{f}(\boldsymbol{x},t)} + \underbrace{\begin{bmatrix} 0.6\cos t \\ 0.6\cos t \\ 0.6\cos t \end{bmatrix}}_{\boldsymbol{d}^m(t)} \tag{42}$$

and

$$\dot{\boldsymbol{y}} = \underbrace{\begin{bmatrix} 0 \\ y_1y_3 \\ y_1y_2 \end{bmatrix}}_{\boldsymbol{g}(\boldsymbol{y})} + \underbrace{\begin{bmatrix} y_2 - y_1 & 0 & 0 \\ -y_1 & y_1 + y_2 & 0 \\ 0 & 0 & -y_3 \end{bmatrix}}_{\boldsymbol{G}(\boldsymbol{y})} \underbrace{\begin{bmatrix} 35 \\ 28 \\ 3 \end{bmatrix}}_{\boldsymbol{\psi}} + \underbrace{\begin{bmatrix} -0.5\sin(\pi y_1) \\ -0.5\sin(2\pi y_2) \\ -0.5\sin(3\pi y_3) \end{bmatrix}}_{\Delta\boldsymbol{g}(\boldsymbol{y},t)} + \underbrace{\begin{bmatrix} -0.6\cos t \\ -0.6\cos t \\ -0.6\cos t \end{bmatrix}}_{\boldsymbol{d}^s(t)} + \begin{bmatrix} u_1(t) \\ u_2(t) \\ u_3(t) \end{bmatrix} \tag{43}$$

Therefore, using Eq. (7), the error dynamics can be expressed as:

$$\begin{cases} \dot{e}_1 = \dot{x}_1 - \dot{y}_1 = \psi_1(e_2 - e_1) + (\theta_1 - \psi_1)(x_2 - x_1) + 0.5\sin(\pi x_1) + 0.5\sin(\pi y_1) + 1.2\cos t - u_1(t) \\ \dot{e}_2 = \dot{x}_2 - \dot{y}_2 = (\psi_2 - \psi_1)e_1 + \psi_2 e_2 + (\theta_2 - \psi_2 + \psi_1)x_1 - (1 + \psi_2)x_2 - x_1x_3 - y_1y_3 + 0.5\sin(2\pi x_2) + 0.5\sin(2\pi y_2) \\ \qquad +1.2\cos t - u_2(t) \\ \dot{e}_3 = \dot{x}_3 - \dot{y}_3 = -\psi_3 e_3 + (\psi_3 - \theta_3)x_3 + x_1x_2 - y_1y_2 + 0.5\sin(3\pi x_3) + 0.5\sin(3\pi y_3) + 1.2\cos t - u_3(t) \end{cases} \tag{44}$$

Consequently, three sliding surfaces are selected as:

$$\begin{cases} s_1 = 10e_1 \\ s_2 = 8e_2 \\ s_3 = 2e_3 \end{cases} \tag{45}$$

Subsequently, according to Eq. (27), the control inputs are taken as:

$$\begin{cases} u_1(t) = \hat{\psi}_1(e_2 - e_1) + (\hat{\theta}_1 - \hat{\psi}_1)(x_2 - x_1) + (\hat{\alpha}_1 + \hat{\beta}_1)\mathrm{sgn}(s_1) + 10\tanh(1000e_1) \\ u_2(t) = (\hat{\psi}_2 - \hat{\psi}_1)e_1 + \hat{\psi}_2 e_2 + (\hat{\theta}_2 - \hat{\psi}_2 + \hat{\psi}_1)x_1 - (1 + \hat{\psi}_2)x_2 - x_1x_3 - y_1y_3 + (\hat{\alpha}_2 + \hat{\beta}_2)\mathrm{sgn}(s_2) + 10\tanh(800e_2) \\ u_3(t) = \hat{\psi}_3 e_3 + (\hat{\psi}_3 - \hat{\theta}_3)x_3 + x_1x_2 - y_1y_2 + (\hat{\alpha}_3 + \hat{\beta}_3)\mathrm{sgn}(s_3) + 10\tanh(200e_3) \end{cases} \tag{46}$$

The Lorenz and Chen systems are started with the initial conditions as follows: $x_1(0) = 6$, $x_2(0) = 3$, $x_3(0) = 7$ and $y_1(0) = 2$, $y_2(0) = 7$, $y_3(0) = 4$.

Fig. 1 illustrates the synchronization errors of the Lorenz and Chen systems, where the control inputs are turned on at $t = 5$ s. As one can see, the synchronization errors converge to the zero, which implies that the chaos synchronization between the Lorenz and Chen systems is realized. The time responses of the update vector parameters $\hat{\boldsymbol{\alpha}}$, $\hat{\boldsymbol{\beta}}$, $\hat{\boldsymbol{\psi}}$ and are depicted in Figs. 2–5, respectively. Obviously, all of the update parameters approach to some constants.

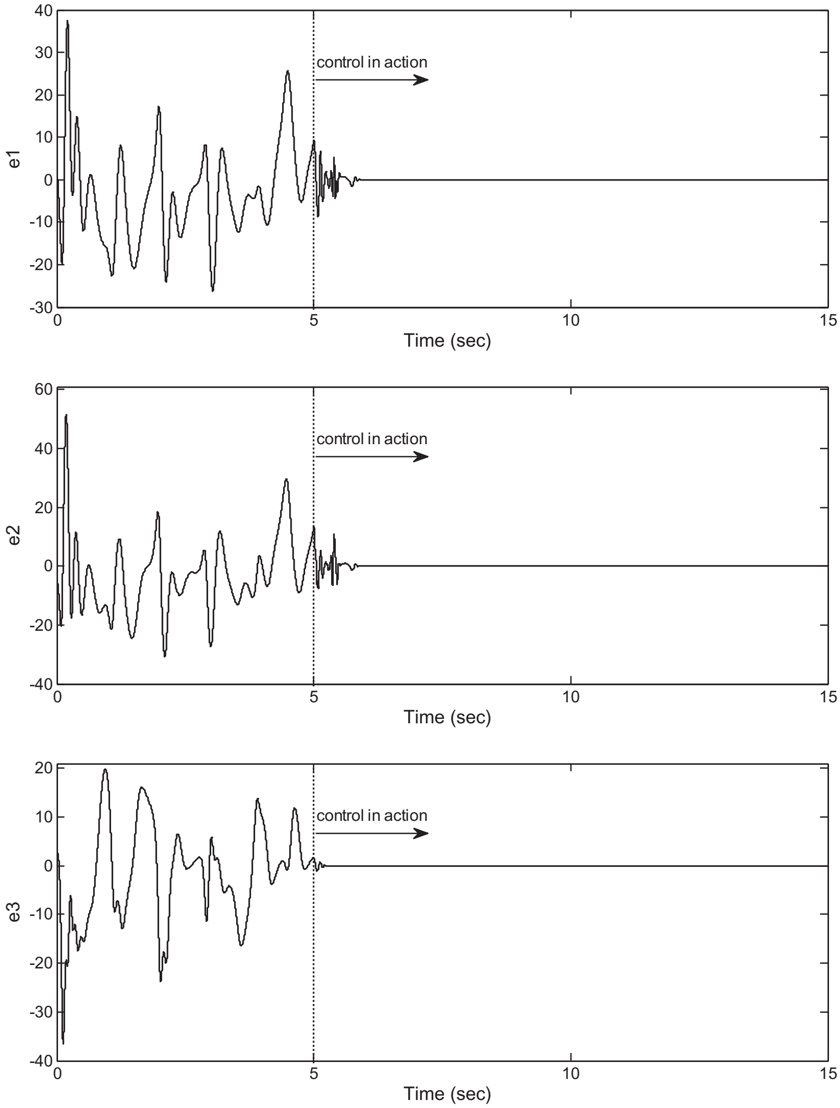

Fig. 1. Synchronization errors of the Lorenz and Chen systems.

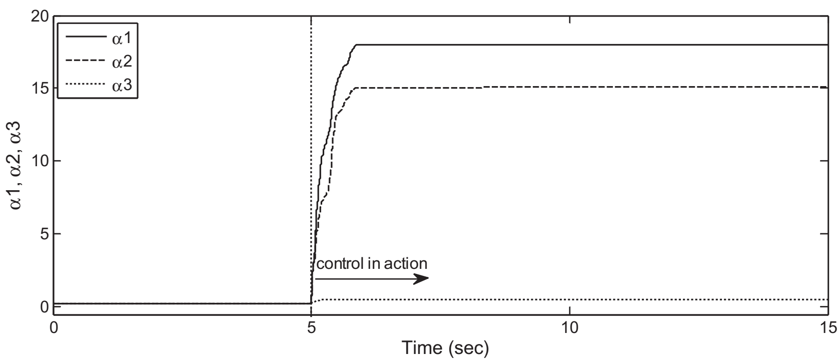

Fig. 2. Time response of the update vector parameter $\hat{\alpha}$.

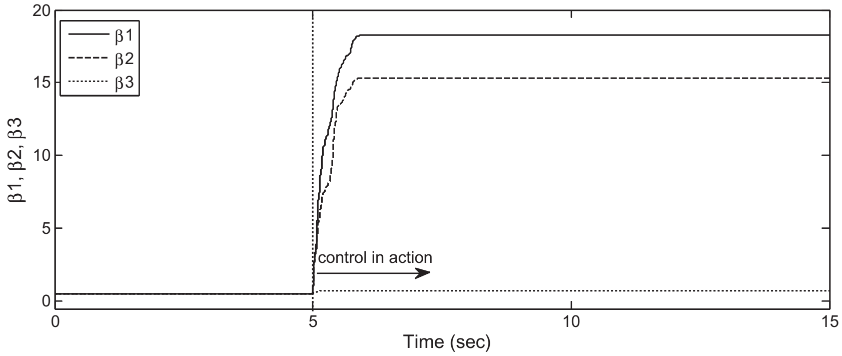

Fig. 3. Time response of the update vector parameter $\hat{\boldsymbol{\beta}}$.

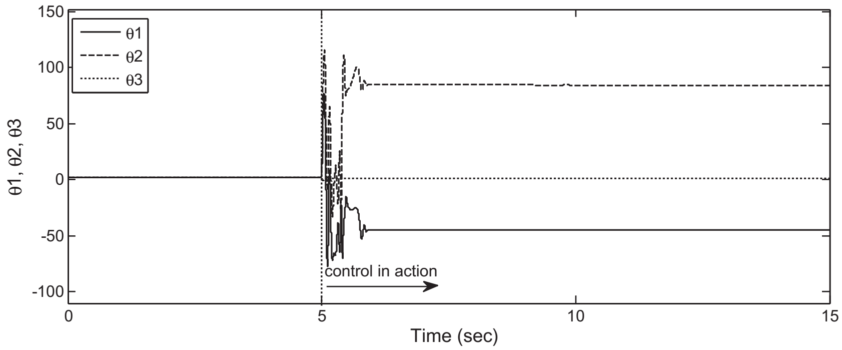

Fig. 4. Time response of the update vector parameter $\hat{\boldsymbol{\theta}}$.

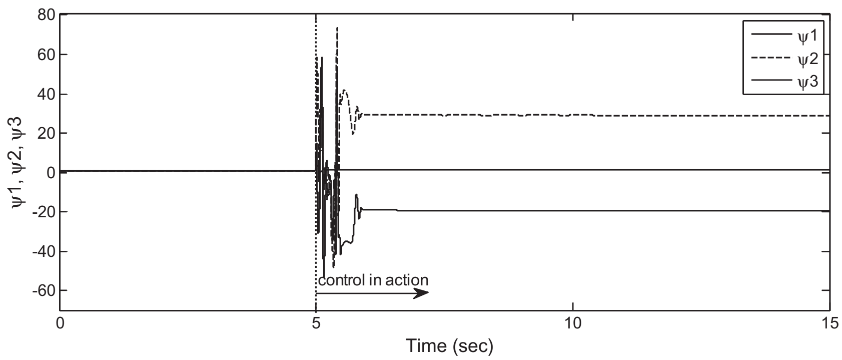

Fig. 5. Time response of the update vector parameter $\hat{\boldsymbol{\psi}}$.

4.2. Chaos synchronization between Chen and Liu systems with uncertainties, external disturbances and unknown parameters

In this case, the Chen and Liu chaotic systems are synchronized using the introduced RASMC. It is supposed that the Chen system is the master system and Liu system is the slave system. These systems can be reformed using Eqs. (1) and (2) as follows:

$$\dot{\boldsymbol{y}} = \underbrace{\begin{bmatrix} 0 \\ y_1y_3 \\ y_1y_2 \end{bmatrix}}_{\boldsymbol{f}(\boldsymbol{y})} + \underbrace{\begin{bmatrix} y_2-y_1 & 0 & 0 \\ -y_1 & y_1+y_2 & 0 \\ 0 & 0 & -y_3 \end{bmatrix}}_{\boldsymbol{F}(\boldsymbol{y})} \underbrace{\begin{bmatrix} 35 \\ 28 \\ 3 \end{bmatrix}}_{\boldsymbol{\theta}} + \underbrace{\begin{bmatrix} 0.5\sin(\pi y_1) \\ 0.5\sin(2\pi y_2) \\ 0.5\sin(3\pi y_3) \end{bmatrix}}_{\Delta\boldsymbol{f}(\boldsymbol{y},t)} + \underbrace{\begin{bmatrix} 0.6\cos t \\ 0.6\cos t \\ 0.6\cos t \end{bmatrix}}_{\boldsymbol{d}^m(t)} \tag{47}$$

and

$$\dot{\boldsymbol{z}} = \underbrace{\begin{bmatrix} 0 \\ -z_1 z_3 \\ 4z_1^2 \end{bmatrix}}_{\boldsymbol{g}(\boldsymbol{z})} + \underbrace{\begin{bmatrix} z_2 - z_1 & 0 & 0 \\ 0 & z_1 & 0 \\ 0 & 0 & -z_3 \end{bmatrix}}_{\boldsymbol{G}(\boldsymbol{z})} \underbrace{\begin{bmatrix} 10 \\ 40 \\ 2.5 \end{bmatrix}}_{\boldsymbol{\psi}} + \underbrace{\begin{bmatrix} -0.5\sin(\pi z_1) \\ -0.5\sin(2\pi z_2) \\ -0.5\sin(3\pi z_3) \end{bmatrix}}_{\Delta\boldsymbol{g}(\boldsymbol{z},t)} + \underbrace{\begin{bmatrix} -0.6\cos t \\ -0.6\cos t \\ -0.6\cos t \end{bmatrix}}_{\boldsymbol{d}^s(t)} + \begin{bmatrix} u_1(t) \\ u_2(t) \\ u_3(t) \end{bmatrix} \tag{48}$$

According to Eq. (7), the error dynamics using can be developed as:

$$\begin{cases} \dot{e}_1 = \dot{y}_1 - \dot{z}_1 = \theta_1(e_2 - e_1) + (\theta_1 - \psi_1)(z_2 - z_1) + 0.5\sin(\pi y_1) + 0.5\sin(\pi z_1) + 1.2\cos t - u_1(t) \\ \dot{e}_2 = \dot{y}_2 - \dot{z}_2 = (\theta_2 - \theta_1)e_1 + \theta_2 y_2 + (\theta_2 - \theta_1 - \psi_2)z_1 + y_1 y_3 + z_1 z_3 + 0.5\sin(2\pi y_2) + 0.5\sin(2\pi z_2) + 1.2\cos t - u_2(t) \\ \dot{e}_3 = \dot{y}_3 - \dot{z}_3 = -\theta_3 e_3 + (\psi_3 - \theta_3)z_3 + y_1 y_2 - 4z_1^2 + 0.5\sin(3\pi y_3) + 0.5\sin(3\pi z_3) + 1.2\cos t - u_3(t) \end{cases} \tag{49}$$

Then, three sliding surfaces are defined as:

$$\begin{cases} s_1 = 20e_1 \\ s_2 = 20e_2 \\ s_3 = 5e_3 \end{cases} \tag{50}$$

Using Eq. (27), the control inputs are computed as:

$$\begin{cases} u_1(t) = \hat{\theta}_1(e_2 - e_1) + (\hat{\theta}_1 - \hat{\psi}_1)(z_2 - z_1) + (\hat{\alpha}_1 + \hat{\beta}_1)\mathrm{sgn}(s_1) + 10\tanh(2000e_1) \\ u_2(t) = (\hat{\theta}_2 - \hat{\theta}_1)e_1 + \hat{\theta}_2 y_2 + (\hat{\theta}_2 - \hat{\theta}_1 - \hat{\psi}_2)z_1 + y_1 y_3 + z_1 z_3 + (\hat{\alpha}_2 + \hat{\beta}_2)\mathrm{sgn}(s_2) + 10\tanh(2000e_2) \\ u_3(t) = -\hat{\theta}_3 e_3 + (\hat{\psi}_3 - \hat{\theta}_3)z_3 + y_1 y_2 - 4z_1^2 + (\hat{\alpha}_3 + \hat{\beta}_3)\mathrm{sgn}(s_3) + 10\tanh(500e_3) \end{cases} \tag{51}$$

The initial conditions for the Chen system are selected as: $y_1(0) = 6$, $y_2(0) = 8$, $y_3(0) = 10$ and for the Liu system are chosen as: $z_1(0) = 2$, $z_2(0) = -2$, $z_3(0) = 5$.

The synchronization errors between the Chen and Liu systems are shown in Fig. 6, while the control inputs are acted at $t = 5$ s. It can be seen that the synchronization errors converge to the zero, which indicates that the Chen and Liu systems are indeed synchronized. The time evolutions of the update vector parameters $\hat{\boldsymbol{\alpha}}$, $\hat{\boldsymbol{\beta}}$, $\hat{\boldsymbol{\theta}}$ and $\hat{\boldsymbol{\psi}}$ are displayed in Figs. 7–10, respectively. It is clear that all update parameters converge to some fixed values.

4.3. Chaos synchronization between Liu and Lorenz systems with uncertainties, external disturbances and unknown parameters

Here, the efficiency of the proposed RASMC is verified by another example of chaotic systems synchronization. In this case, the Liu system drives the Lorenz system. The reformulated form of the Liu and Lorenz systems are presented by

$$\dot{\boldsymbol{z}} = \underbrace{\begin{bmatrix} 0 \\ -z_1 z_3 \\ 4z_1^2 \end{bmatrix}}_{\boldsymbol{f}(\boldsymbol{z})} + \underbrace{\begin{bmatrix} z_2 - z_1 & 0 & 0 \\ 0 & z_1 & 0 \\ 0 & 0 & -z_3 \end{bmatrix}}_{F(\boldsymbol{z})} \underbrace{\begin{bmatrix} 10 \\ 40 \\ 2.5 \end{bmatrix}}_{\boldsymbol{\theta}} + \underbrace{\begin{bmatrix} 0.5\sin(\pi z_1) \\ 0.5\sin(2\pi z_2) \\ 0.5\sin(3\pi z_3) \end{bmatrix}}_{\Delta\boldsymbol{f}(\boldsymbol{z},t)} + \underbrace{\begin{bmatrix} 0.6\cos t \\ 0.6\cos t \\ 0.6\cos t \end{bmatrix}}_{\boldsymbol{d}^m(t)} \tag{52}$$

and

$$\dot{\boldsymbol{x}} = \underbrace{\begin{bmatrix} 0 \\ -x_1 x_3 - x_2 \\ x_1 x_2 \end{bmatrix}}_{\boldsymbol{g}(\boldsymbol{x})} + \underbrace{\begin{bmatrix} x_2 - x_1 & 0 & 0 \\ 0 & x_1 & 0 \\ 0 & 0 & -x_3 \end{bmatrix}}_{\boldsymbol{G}(\boldsymbol{x})} \underbrace{\begin{bmatrix} 10 \\ 28 \\ 8/3 \end{bmatrix}}_{\boldsymbol{\psi}} + \underbrace{\begin{bmatrix} -0.5\sin(\pi x_1) \\ -0.5\sin(2\pi x_2) \\ -0.5\sin(3\pi x_3) \end{bmatrix}}_{\Delta\boldsymbol{g}(\boldsymbol{x},t)} + \underbrace{\begin{bmatrix} 0.6\cos t \\ 0.6\cos t \\ 0.6\cos t \end{bmatrix}}_{\boldsymbol{d}^s(t)} + \begin{bmatrix} u_1(t) \\ u_2(t) \\ u_3(t) \end{bmatrix} \tag{53}$$

The error dynamics using Eq. (7) can be presented as:

$$\begin{cases} \dot{e}_1 = \dot{z}_1 - \dot{x}_1 = \theta_1(e_2 - e_1) + (\theta_1 - \psi_1)(x_2 - x_1) + 0.5\sin(\pi z_1) + 0.5\sin(\pi x_1) + 1.2\cos t - u_1(t) \\ \dot{e}_2 = \dot{z}_2 - \dot{x}_2 = \theta_2 e_1 + (\theta_2 - \psi_2)x_1 - z_1 z_3 + x_1 x_3 + x_2 + 0.5\sin(2\pi z_2) + 0.5\sin(2\pi x_2) + 1.2\cos t - u_2(t) \\ \dot{e}_3 = \dot{z}_3 - \dot{x}_3 = -\theta_3 e_3 + (\psi_3 - \theta_3)x_3 + 4z_1^2 - x_1 x_2 + 0.5\sin(3\pi z_3) + 0.5\sin(3\pi x_3) + 1.2\cos t - u_3(t) \end{cases} \tag{54}$$

Subsequently, three sliding surfaces are chosen as:

$$\begin{cases} s_1 = 15e_1 \\ s_2 = 15e_2 \\ s_3 = 10e_3 \end{cases} \tag{55}$$

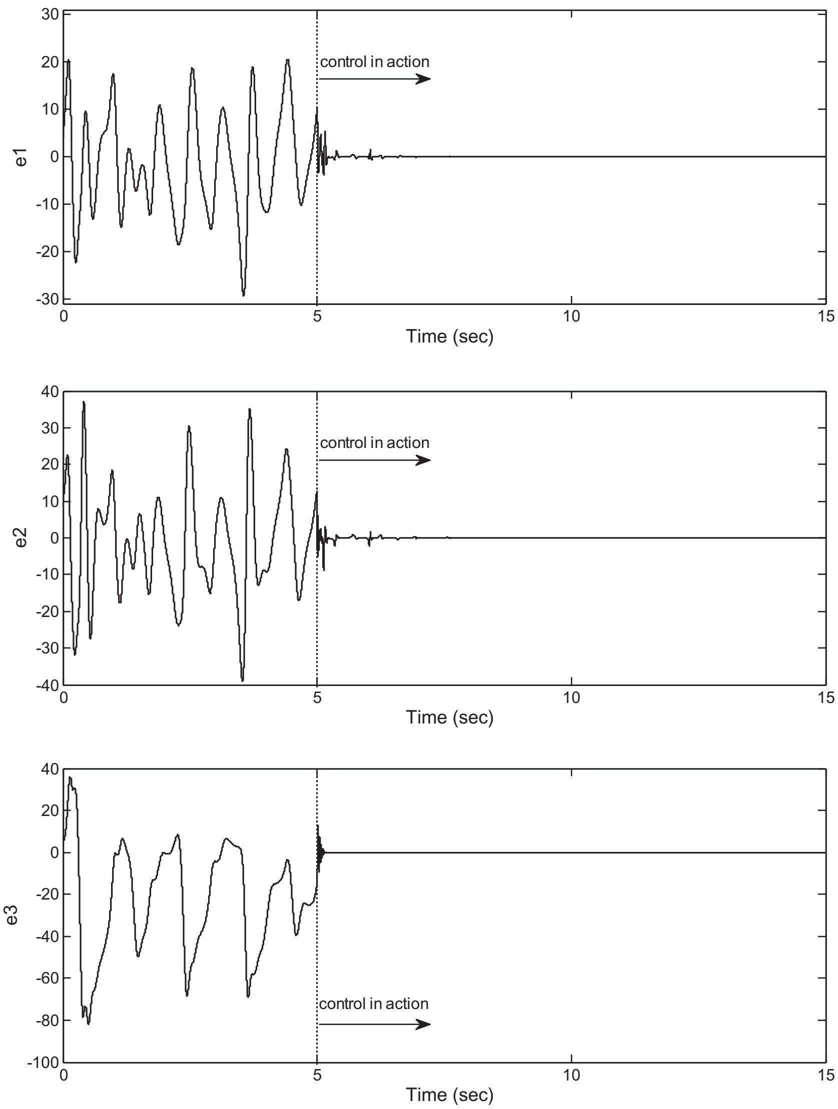

Fig. 6. Synchronization errors of the Chen and Liu systems.

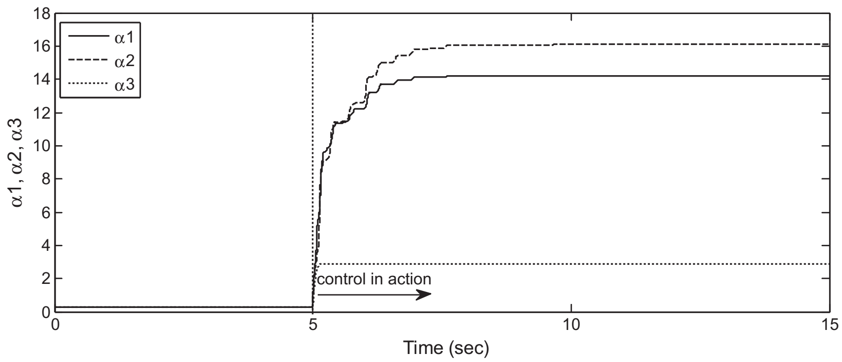

Fig. 7. Time response of the update vector parameter $\hat{\alpha}$.

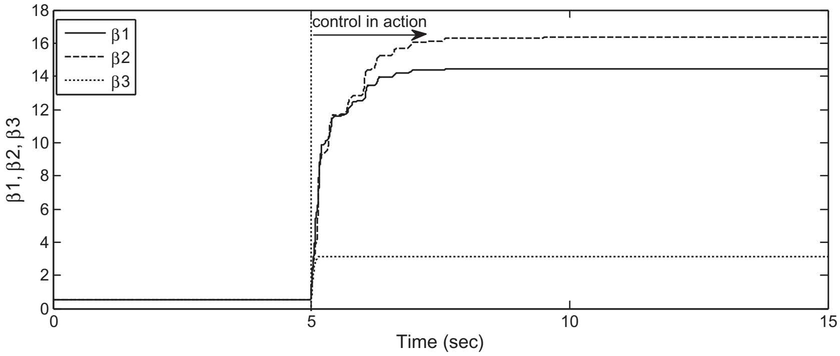

Fig. 8. Time response of update vector parameter $\hat{\boldsymbol{\beta}}$.

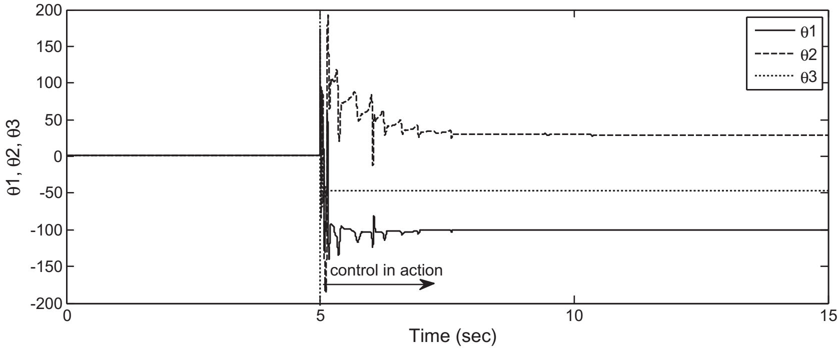

Fig. 9. Time response of the update vector parameter $\hat{\boldsymbol{\theta}}$.

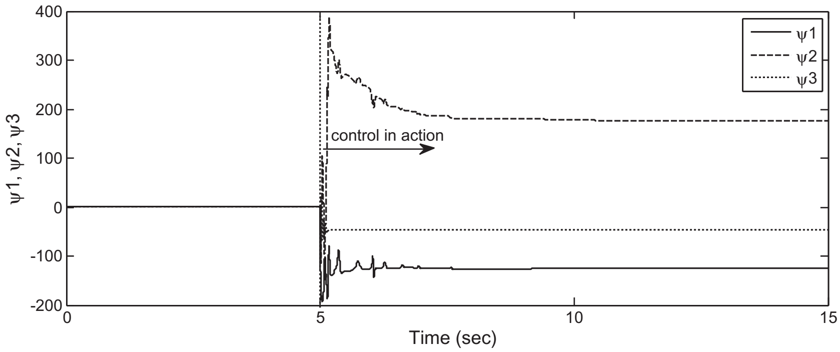

Fig. 10. Time response of the update vector parameter $\hat{\boldsymbol{\psi}}$.

Then, the control inputs are derived using the Eq. (27) as follows:

$$\begin{cases} u_1(t) = \hat{\theta}_1(e_2 - e_1) + (\hat{\theta}_1 - \hat{\psi}_1)(x_2 - x_1) + (\hat{\alpha}_1 + \hat{\beta}_1)sgn(s_1) + 10\tanh(1500e_1) \\ u_2(t) = \hat{\theta}_2 e_1 + (\hat{\theta}_2 - \hat{\psi}_2)x_1 - z_1 z_3 + x_1 x_3 + x_2 + (\hat{\alpha}_2 + \hat{\beta}_2)sgn(s_2) + 10\tanh(1500e_2) \\ u_3(t) = -\hat{\theta}_3 e_3 + (\hat{\psi}_3 - \hat{\theta}_3)x_3 + 4z_1^2 - x_1 x_2 + (\hat{\alpha}_3 + \hat{\beta}_3)sgn(s_3) + 10\tanh(1000e_3) \end{cases} \tag{56}$$

The Liu system is initialized with $z_1(0) = 5$, $z_2(0) = -3$, $z_3(0) = 10$ and the Lorenz system is started with $x_1(0) = 10$, $x_2(0) = 2$, $x_3(0) = 4$.

Fig. 11 reveals the synchronization errors between the Liu and Lorenz systems, where the control inputs are activated at $t = 5$ s. It can be observed that the synchronization errors regulate to the zero, which implies that the synchronization objective is achieved absolutely. The time responses of the update vector parameters $\hat{\boldsymbol{\alpha}}$, $\hat{\boldsymbol{\beta}}$, $\hat{\boldsymbol{\theta}}$ and $\hat{\boldsymbol{\psi}}$ are appeared in Figs. 12–15, respectively. One can see that the update parameters are bounded.

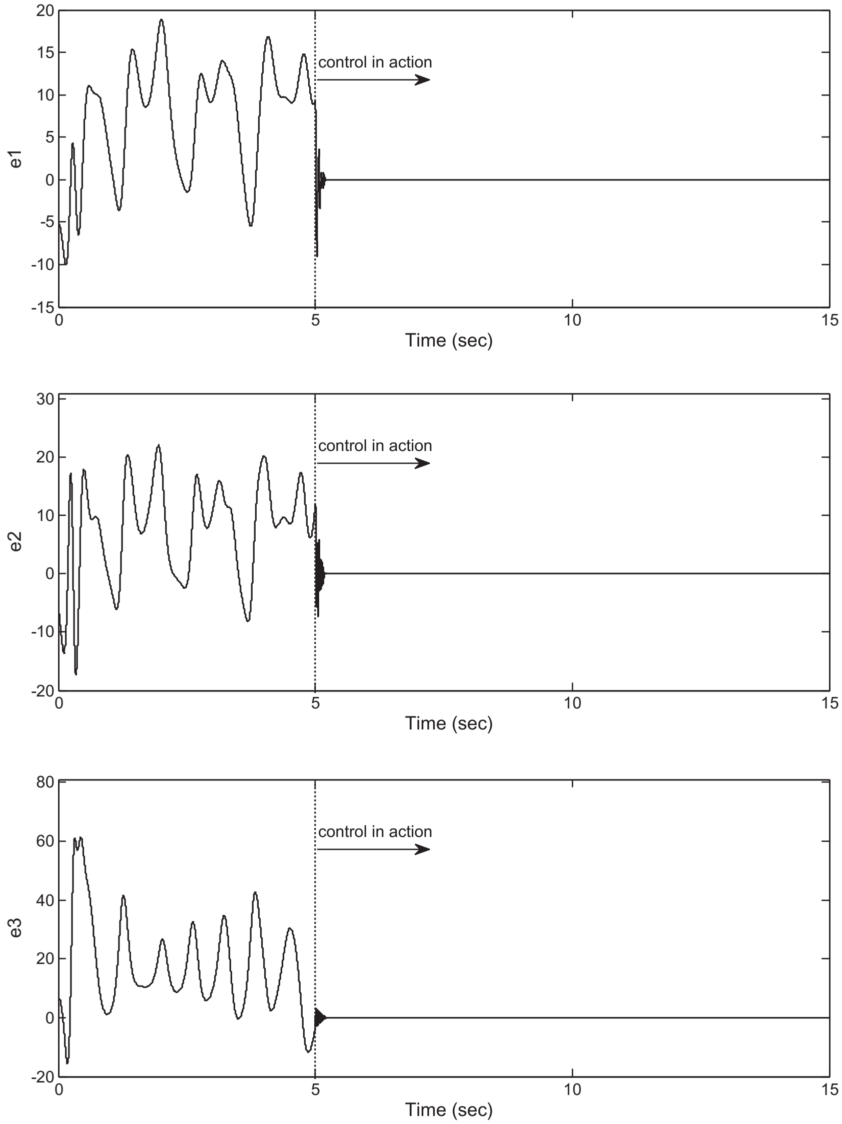

Fig. 11. Synchronization errors of the Liu and Lorenz systems.

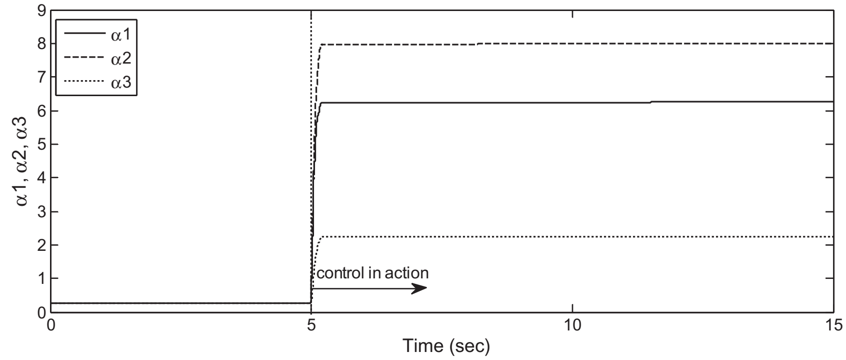

Fig. 12. Time response of the update vector parameter $\hat{\boldsymbol{\alpha}}$.

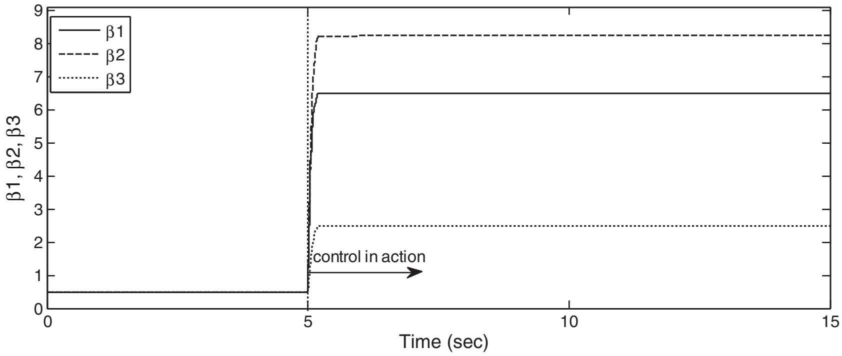

Fig. 13. Time response of the update vector parameter $\hat{\boldsymbol{\beta}}$.

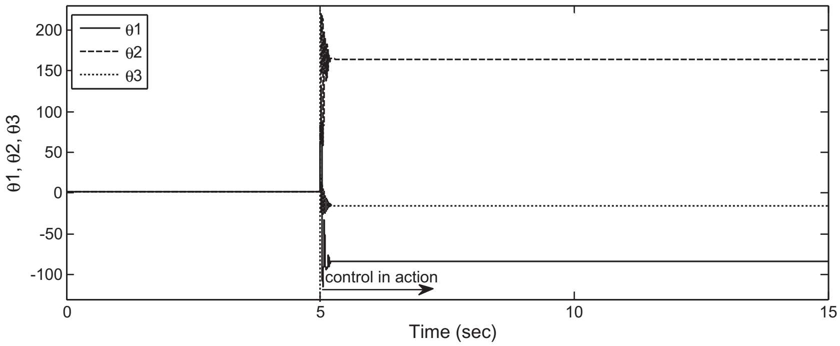

Fig. 14. Time response of the update vector parameter $\hat{\boldsymbol{\theta}}$.

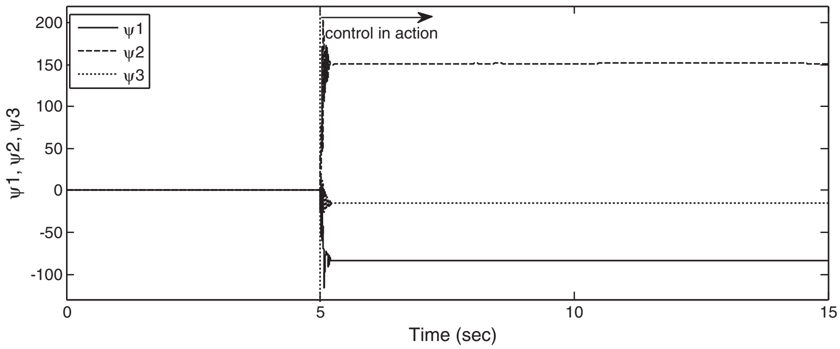

Fig. 15. Time response of the update vector parameter $\hat{\boldsymbol{\psi}}$.

5. Conclusions

In this paper, the problem of practical synchronization of chaotic systems is investigated. In real world applications, there are always some uncertainties and external disturbances in the system dynamics. Also, in practical or experimental situations, the system parameters are inevitably disturbed by external inartificial factors, such as environment temperature, voltage fluctuation, mutual interfere between components, and cannot be exactly known in advance. The synchronization may be destroyed and even broken with the effects of these uncertainties. In this paper, therefore, the effects of the model uncertainties, external disturbances and unknown parameters in synchronizing two different chaotic systems are fully taken into account. An adaptive sliding mode controller is designed to robustly synchronize two different uncertain chaotic systems with unknown parameters. Some numerical simulations are presented to show the applicability and feasibility of the proposed scheme.

It is worth noting that three remarkable features of the proposed approach are: (1) it is robust with respect to the model uncertainties, external disturbances and unknown parameters; (2) it can be easily realized and implemented in real world applications (for example in secure communication applications) without requiring the bounds of the model uncertainties, external disturbances and unknown parameters to be known in advance; (3) it is well applicable for practical synchronization of two different (or identical) chaotic systems even when both master and slave chaotic systems are disturbed by the model uncertainties, external disturbances and unknown parameters.

References

[1] Chen G, Dong X. From chaos to order: methodologies, perspectives and applications. Singapore: World Scientific; 1998.
[2] Nayfeh AH. Applied nonlinear dynamics. New York: Wiley; 1995.
[3] Kapitaniak T. Chaotic oscillations in mechanical systems. New York: Manchester University Press; 1991.
[4] Wang H, Han Z, Xie Q, Zhang W. Finite-time chaos control via nonsingular terminal sliding mode control. Commun Nonlinear Sci Numer Simulat 2009;14:2728–33.
[5] Xiang W, Huangpu Y. Second-order terminal sliding mode controller for a class of chaotic systems with unmatched uncertainties. Commun Nonlinear Sci Numer Simulat 2010;15:3241–7.
[6] Wang H, Han Z, Xie Q, Zhang W. Sliding mode control for chaotic systems based on LMI. Commun Nonlinear Sci Numer Simulat 2009;14:1410–7.
[7] Fuh C. Optimal control of chaotic systems with input saturation using an input-state linearization scheme. Commun Nonlinear Sci Numer Simulat 2009;14:3424–31.
[8] Grzybowski JMV, Rafikov M, Balthazar JM. Synchronization of the unified chaotic system and application in secure communication. Commun Nonlinear Sci Numer Simulat 2009;14:2793–806.
[9] Rafikov M, Balthazar JM. On control and synchronization in chaotic and hyperchaotic systems via linear feedback control. Commun Nonlinear Sci Numer Simulat 2008;13:1246–55.
[10] Bowong S. Adaptive synchronization between two different chaotic dynamical systems. Commun Nonlinear Sci Numer Simulat 2007;12:976–85.
[11] Lazzouni SA, Bowong S, Kakmeni FMM, Cherki B. An adaptive feedback control for chaos synchronization of nonlinear systems with different order. Commun Nonlinear Sci Numer Simulat 2007;12:568–83.
[12] Chen H, Sheu G, Lin Y, Chen C. Chaos synchronization between two different chaotic systems via nonlinear feedback control. Nonlinear Anal 2009;70:4393–401.
[13] Wang B, Wen G. On the synchronization of a class of chaotic systems based on backstepping method. Phys Lett A 2007;370:35–9.
[14] Yassen MT. Controlling, synchronization and tracking chaotic Liu system using active backstepping design. Phys Lett A 2007;360:582–7.
[15] Wang F, Liu C. Synchronization of unified chaotic system based on passive control. Physica D 2007;225:55–60.
[16] Lee SM, Ji DH, Park JH, Won SC. $H\infty$ synchronization of chaotic systems via dynamic feedback approach. Phys Lett A 2008;372:4905–12.
[17] Yau H, Shieh C. Chaos synchronization using fuzzy logic controller. Nonlinear Anal: RWA 2008;9:1800–10.
[18] Chang W. PID control for chaotic synchronization using particle swarm optimization. Chaos Soliton Fract 2009;39:910–7.
[19] Sun Y. Chaos synchronization of uncertain Genesio–Tesi chaotic systems with deadzone nonlinearity. Phys Lett A 2009;373:3273–6.
[20] Yan J, Yang Y, Chiang T, Chen C. Robust synchronization of unified chaotic systems via sliding mode control. Chaos Soliton Fract 2007;34:947–54.
[21] Jianwen F, Ling H, Chen X, Austin F, Geng W. Synchronizing the noise-perturbed Genesio chaotic system by sliding mode control. Commun Nonlinear Sci Numer Simulat 2010;15:2546–51.
[22] Yau H. Design of adaptive sliding mode controller for chaos synchronization with uncertainties. Chaos Soliton Fract 2004;22:341–7.
[23] Zhang H, Ma X, Liu W. Synchronization of chaotic systems with parametric uncertainty using active sliding mode control. Chaos Soliton Fract 2004;21:1249–57.
[24] Feki M. Sliding mode control and synchronization of chaotic systems with parametric uncertainties. Chaos Soliton Fract 2009;41:1390–400.
[25] Lin C, Peng Y, Lin M. CMAC-based adaptive backstepping synchronization of uncertain chaotic systems. Chaos Soliton Fract 2009;42:981–8.
[26] Ahmadi AA, Majd VJ. Robust synchronization of a class of uncertain chaotic systems. Chaos Soliton Fract 2009;42:1092–6.
[27] Asheghan MM, Beheshti MTH. An LMI approach to robust synchronization of a class of chaotic systems with gain variations. Chaos Soliton Fract 2009;42:1106–11.
[28] Zhang H, Ma X. Synchronization of uncertain chaotic systems with parameters perturbation via active control. Chaos Soliton Fract 2004;21:39–47.
[29] Cai N, Jing Y, Zhang S. Modified projective synchronization of chaotic systems with disturbances via active sliding mode control. Commun Nonlinear Sci Numer Simulat 2010;15:1613–20.
[30] Haeri M, Tavazoei MS, Naseh MR. Synchronization of uncertain chaotic systems using active sliding mode control. Chaos Soliton Fract 2007;33:1230–9.
[31] Kebriaei H, Yazdanpanah MJ. Robust adaptive synchronization of different uncertain chaotic systems subject to input nonlinearity. Commun Nonlinear Sci Numer Simulat 2010;15:430–41.
[32] Chen C. Quadratic optimal neural fuzzy control for synchronization of uncertain chaotic systems. Expert Syst Appl 2009;36:11827–35.
[33] Yan J, Hung M, Liao T. Adaptive sliding mode control for synchronization of chaotic gyros with fully unknown parameters. J Sound Vibr 2006;298:298–306.
[34] Li W, Chang K. Robust synchronization of drive-response chaotic systems via adaptive sliding mode control. Chaos Soliton Fract 2009;39:2086–92.
[35] Wang H, Han Z, Xie Q, Zhang W. Finite-time chaos synchronization of unified chaotic system with uncertain parameters. Commun Nonlinear Sci Numer Simulat 2009;14:2239–47.
[36] Salarieh H, Alasty A. Adaptive chaos synchronization in Chua's systems with noisy parameters. Math Comput Simulat 2008;79:233–41.
[37] Zhang G, Liu Z, Zhang J. Adaptive synchronization of a class of continuous chaotic systems with uncertain parameters. Phys Lett A 2008;372:447–50.
[38] Shen L, Wang M. Robust synchronization and parameter identification on a class of uncertain chaotic systems. Chaos Soliton Fract 2008;38:106–11.
[39] Ma J, Zhang A, Xia Y, Zhang L. Optimize design of adaptive synchronization controllers and parameter observers in different hyperchaotic systems. Appl Math Comput 2010;215:3318–26.
[40] El-Gohary A. Optimal synchronization of Rossler system with complete uncertain parameters. Chaos Soliton Fract 2006;27:345–55.
[41] El-Gohary A, Sarhan A. Optimal control and synchronization of Lorenz system with complete unknown parameters. Chaos Soliton Fract 2006;30:1122–32.
[42] Zhang L, Huang L, Zhang Z, Wang Z. Fuzzy adaptive synchronization of uncertain chaotic systems via delayed feedback control. Phys Lett A 2008;372:6082–6.
[43] Kim J, Park C, Kim E, Park M. Fuzzy adaptive synchronization of uncertain chaotic systems. Phys Lett A 2005;334:295–305.
[44] Hwang E, Hyun C, Kim E, Park M. Fuzzy model based adaptive synchronization of uncertain chaotic systems: robust tracking control approach. Phys Lett A 2009;373:1935–9.
[45] Huang J. Chaos synchronization between two novel different hyperchaotic systems with unknown parameters. Nonlinear Anal 2008;69:4174–81.
[46] Yassen MT. Adaptive synchronization of two different uncertain chaotic systems. Phys Lett A 2005;337:335–41.
[47] Chen X, Lu J. Adaptive synchronization of different chaotic systems with fully unknown parameters. Phys Lett A 2007;364:123–8.
[48] Zhang H, Huang W, Wang Z, Chai T. Adaptive synchronization between two different chaotic systems with unknown parameters. Phys Lett A 2006;350:363–6.
[49] Salarieh H, Shahrokhi M. Adaptive synchronization of two different chaotic systems with time varying unknown parameters. Chaos Soliton Fract 2008;37:125–36.
[50] Yan J, Hung M, Chiang T, Yang Y. Robust synchronization of chaotic systems via adaptive sliding mode control. Phys Lett A 2006;356:220–5.

[51] Wang C, Ge SS. Adaptive synchronization of uncertain chaotic systems via backstepping design. Chaos Soliton Fract 2001;12:1199–206.
[52] Utkin V. Sliding modes in control and optimization. Berlin: Springer Verlag; 1992.
[53] Khalil H-K. Nonlinear system. third ed. New Jersey: Prentice Hall; 2002.
[54] Lorenz E. Deterministic nonperiodic flow. J Atmos Sci 1963;20:130–41.
[55] Chen G, Ueta T. Yet another chaotic attractor. Int J Bifur Chaos 1999;9:1465–6.
[56] Liu C, Liu T, Liu L, Liu K. A new chaotic attractor. Chaos Soliton Fract 2004;22:1031–8.